NanoPen: Dynamic, Low-Power, and Light-Actuated Patterning of Nanoparticles

Arash Jamshidi,[†] Steven L. Neale,[†] Kyoungsik Yu,[†] Peter J. Pauzauskie,[‡] Peter James Schuck,[§] Justin K. Valley,[†] Hsan-Yin Hsu,[†] Aaron T. Ohta,[†,‖] and Ming C. Wu*,[†]

Department of Electrical Engineering and Computer Sciences, University of California, Berkeley, California 94720, Chemical Sciences Division, Lawrence Livermore National Laboratory, Berkeley, California 94720, and Molecular Foundry, Lawrence Berkeley National Laboratory, Berkeley, California 94720

ABSTRACT

We introduce NanoPen, a novel technique for low optical power intensity, flexible, real-time reconfigurable, and large-scale light-actuated patterning of single or multiple nanoparticles, such as metallic spherical nanocrystals, and one-dimensional nanostructures, such as carbon nanotubes. NanoPen is capable of dynamically patterning nanoparticles over an area of thousands of square micrometers with light intensities <10 W/cm^2 (using a commercial projector) within seconds. Various arbitrary nanoparticle patterns and arrays (including a 10 × 10 array covering a 0.025 mm^2 area) are demonstrated using this capability. One application of NanoPen is presented through the creation of surface-enhanced Raman spectroscopy hot-spots by patterning gold nanoparticles of 90 nm diameter with enhancement factors exceeding 10^7 and picomolar concentration sensitivities.

The ability to pattern nanostructures has important applications in medical diagnosis,[1,2] sensing,[3] nano- and optoelectronic device fabrication,[4,5] nanostructure synthesis,[6] and photovoltaics.[7] Several techniques such as dip-pen nanolithography,[8−13] nanofabrication,[14] contact printing,[15−18] self-assembly,[19,20] and Langmuir−Blodgett[21] have been used to pattern nanostructures. However, these techniques lack the capability to create real-time reconfigurable patterns without the use of complicated instrumentation or processing steps. Various optical patterning techniques[22−26] have tried to overcome this challenge. Optical patterning of nanoparticles has been achieved previously by actuating an indium−tin oxide (ITO) layer as a photoconductive material and generating local current densities to concentrate the nanoparticles. However, these methods suffer from a slow patterning process[22] (several minutes to hours) or they require very high optical intensities[23] (~10^5 W/cm^2) to pattern the nanostructures. These limitations prevent the widespread application of such techniques. Alternatively, optical tweezers have been used to manipulate and permanently assemble nanostructures

onto the substrate.[24,25] Moreover, optical tweezers have been combined with local heating of nanoparticles to create convective flows for collection and patterning of particles.[26] However, optical tweezers are also limited to using very high optical intensities (~10^7 W/cm^2) and high numerical aperture objectives, which limits the ease of operation, reduces the available working area, and potentially damages the nanoparticles.[24]

Optoelectronic tweezers (OET)[27] work based on the principles of an optically induced dielectrophoresis (DEP)[28] force and have been used extensively to manipulate, separate, and organize microparticles[27,29] and nanostructures.[30] In addition to the DEP force, two other major electrokinetic forces have been observed and studied in the OET device,[31] namely, light-actuated ac electroosmosis (LACE)[32,33] and electrothermal (ET)[34] flow. In this paper, we report the novel use of OET optofluidic platform for "directly writing" patterns of nanoparticles. We call this novel technique NanoPen. NanoPen uses various electrokinetic forces (DEP, LACE, and ET) to collect and permanently immobilize nanoparticles on the OET surface. NanoPen can be operated to collect and immobilize single and multiple nanoparticles such as spherical metallic nanocrystals and one-dimensional nanostructures such as multiwall carbon nanotubes. We would like to note that the name NanoPen refers to a method

* Corresponding author: wu@eecs.berkeley.edu.
† Department of Electrical Engineering and Computer Sciences, University of California, Berkeley.
‡ Chemical Sciences Division, Lawrence Livermore National Laboratory.
§ Molecular Foundry, Lawrence Berkeley National Laboratory.
‖ Current address: Department of Electrical Engineering, University of Hawai'i at Mānoa, Honolulu, HI 96822.
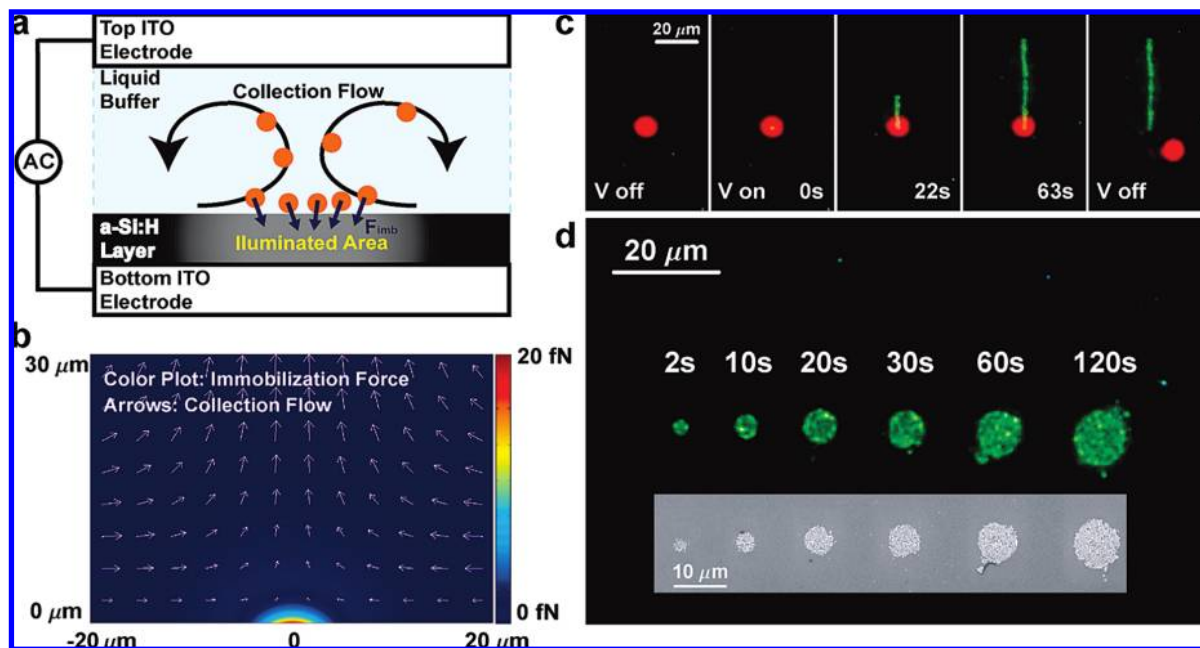
Figure 1. The NanoPen mechanism. (a) OET optofluidic platform used to realize the NanoPen process. The device consists of a bottom glass substrate covered with a 300 nm thick ITO layer on top of which a 1 μm layer of hydrogenated amorphous silicon (a-Si:H) is deposited. The liquid layer containing the nanoparticles is sandwiched between the bottom surface and a top ITO glass electrode using a 100 μm spacer. The collection flow collects the particles toward the illuminated area and the immobilization force (F_{imb}) patterns the particles on the surface. (b) Finite-element simulation of the NanoPen process. The arrows indicate the collection flow which is a combination of the electrothermal (ET) flow and light-actuated ac electroosmosis (LACE) flow. The immobilization force consists mainly of the dielectrophoresis (DEP) force. (c) Real-time patterning of 90 nm diameter gold nanoparticles by translating the stage while patterning the particles in the illuminated area. The red spot is the patterning beam and the green areas indicate the patterned nanoparticles. In the beginning the voltage is off and no particles are immobilized, once the voltage is turned on, the nanoparticles are collected and permanently patterned in the illuminated area. The stage is manually transported, leaving a trace of the nanoparticles behind. Once the patterning is complete, the voltage is turned off and the patterning process stops. (d) Increasing the exposure time expands the patterned area and density of particles within the illuminated region as indicated for 2−120s exposure times. The inset shows the scanning electron microscopy image of the patterned spots.

for patterning nanoparticles (a Nanoparticle Pen) and does not mean nanoscale positioning accuracy.

Figure 1a shows the device structure for OET nanopatterning optofluidic platform. The OET device consists of a top ITO transparent electrode and a bottom ITO electrode on top of which there is a 1 μm layer of hydrogenated amorphous silicon (a-Si:H). The nanoparticles of interest, such as metallic nanocrystals, carbon nanotubes, and nanowires are dispersed in a KCl/DI (deionized) water solution with 1−10 mS/m conductivity which is sandwiched between the top and the bottom electrode layers. There is an ac voltage applied between the two ITO electrodes, with 10−20 peak-to-peak voltage and 10−100 kHz frequency. To actuate the OET device, an optical pattern is projected on the a-Si:H layer, by using either a laser source, a spatial light modulator, or a commercial projector. The light pattern generates electron−hole pairs in the a-Si:H layer, locally increasing the conductivity of the photoconductive material, and transferring the ac voltage to the liquid layer only in the area that the light pattern is present. This will create a nonuniform field distribution in the liquid layer which can interact with particles in the liquid, attracting or repelling them from areas of high electric field intensity according to the DEP principle.

In addition to the DEP force, the presence of the nonuniform electric field and the heat generated by absorption of the light pattern in the a-Si:H result in two other major

electrokinetic forces: first, LACE flow;[32,33,35] second, ET flow.[31,34] LACE flow is created due to the interaction of the lateral component of the electric field with the electrical double layer on the a-Si:H surface and is observed mainly at frequencies below 50 kHz. On the other hand, the absorption of the light in the a-Si:H creates a local heat gradient which in turn creates a gradient in permittivity and conductivity of the liquid layer, generating dielectrophoretic forces on the liquid layer. This force drives the liquid in a vortex flow pattern around the illuminated area; this flow is called the electrothermal (ET) flow. Figure 1b depicts finite-element simulation (using COMSOL Multiphysics) of these electrokinetic forces in the OET chamber for an applied voltage of 20 V_{pp} at 10 kHz, with 1 mS/m liquid conductivity. The DEP[28] force is modeled using

$$F_{DEP} = 2\pi r^3 \varepsilon_m \text{Re}\{K\}\nabla E^2$$

where r is the radius of the particle, ε_m is the permittivity of the media, $\text{Re}\{K\}$ is the real part of the Clausius−Mossotti, and E is the electric field; LACE flow is modeled by calculating the slip velocity[36] due to the interaction of the lateral component of the electric field with the electrical double layer on a-Si:H surface, $v_{Slip} = -(\varepsilon_m \xi E_t)/(\eta)$, where ζ is the zeta potential of the electrical double layer and E_t is the lateral component of the electric field; the ET flow can be modeled by calculating the temperature gradient ∇T due
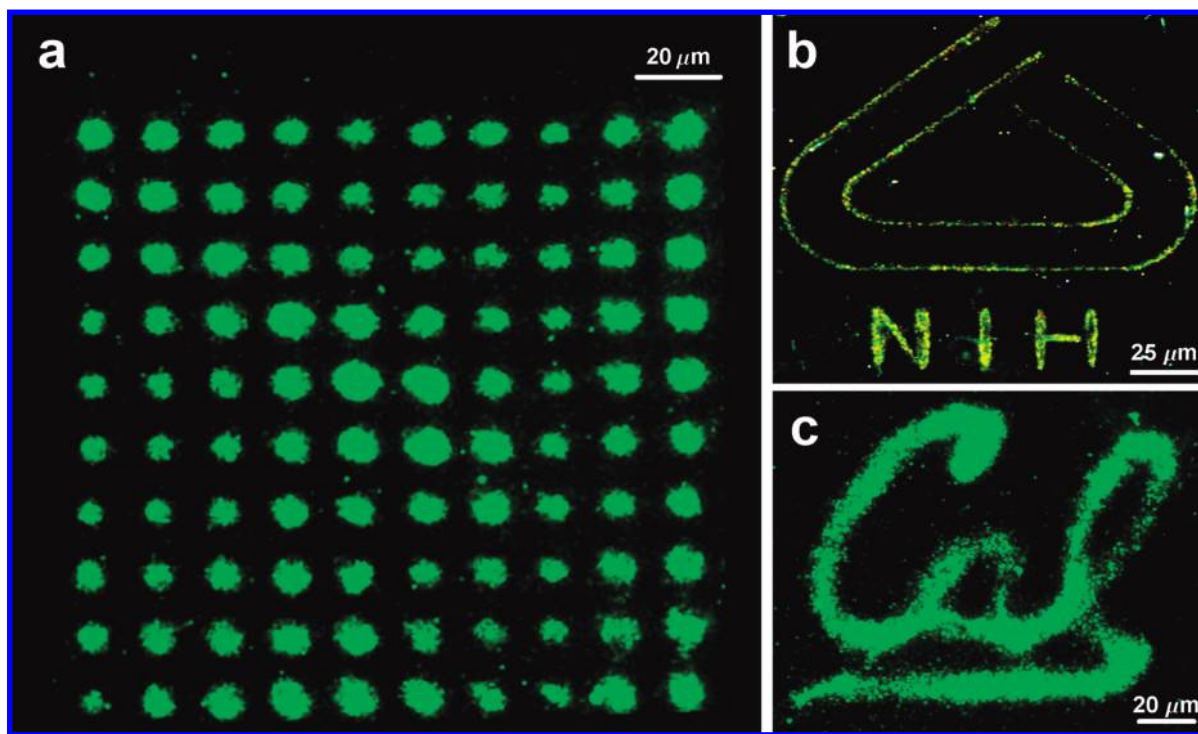
Figure 2. Large area patterning of nanoparticles using NanoPen. Patterning of 90 nm diameter gold nanoparticles in the form of (a) a 10 × 10 array, over 150 × 140 μm^2, (b) "NIH" logo over 160 × 140 μm^2, and (c) "CAL" logo over 140 × 110 μm^2, all using a commercial light projector (<10 W/cm^2 light intensity).

to Joule heating in a-Si:H ($\sigma_{aSi}E^2$) which results in a gradient in permittivity and conductivity of the liquid. The interaction of these gradients with the nonuniform electric field, creates a body force on the liquid given by[34]

$$\langle f_{ET} \rangle = \frac{1}{2}\mathrm{Re}\left[\left(\frac{\sigma_m \varepsilon_m}{\sigma_m + i\omega\varepsilon_m}(\kappa_\varepsilon - \kappa_\sigma)\right)(\nabla T \cdot E)E^*\right] - \frac{1}{2}|E|^2 \kappa_\varepsilon \varepsilon_m \nabla T$$

where σ_m and ε_m are the liquid conductivity and permittivity, respectively, and κ_ε and κ_σ are the permittivity and conductivity gradients generated due to the temperature gradient, ∇T.

The NanoPen mechanism benefits from the combination of these electrokinetic forces generated in the OET optofluidic platform. In particular, there are two distinct forces that lead to light-actuated patterning of nanoparticles: a collection force responsible for collecting the particles from long-range (over 100 μm) distances and concentrating them in the light spot and an immobilization force which strongly attracts the particles (with up to 0.1 pN forces) and immobilizes them on the OET surface. The collection force benefits from DEP force attraction of particles over the short range and LACE and ET flow-based collection of the particles over the longer range. The immobilization force which is responsible for attracting the particles to the surface is mainly dominated by the DEP force but is also affected by electrophoretic forces due to the particles surface charges.

Figure 1c shows NanoPen immobilization and patterning of 90 nm diameter spherical gold nanoparticles (purchased from Nanopartz Inc.[37]) dispersed in a 5 mS/m solution of KCl and DI water with ~10^{11} particles/mL concentration.

In the beginning, there is no voltage applied to the device and the nanoparticles undergo Brownian motion. Once the voltage is applied (20 V_{pp} at 50 kHz), the nanoparticles are collected in the center of the light spot (continuous wave 633 nm diode laser, 100 μW) and are immobilized on the OET bottom surface. The stage is then manually transported leaving a trace of gold nanoparticles in the illuminated area on the OET surface. Once the immobilization process is complete, the liquid solution can be removed without damaging the patterned structure. The patterned surface remains intact after multiple rinsing and drying steps. In addition, using a diluted nanoparticle solution, NanoPen is capable of patterning single nanoparticles as depicted in Figure S1 of the Supporting Information for patterning a single 90 nm diameter spherical gold nanoparticle. We have also demonstrated that NanoPen is capable of patterning one-dimensional nanostructures such as multiwall carbon nanotubes (see Figure S2 in the Supporting Information) as well as semiconducting and metallic nanowires (see Figure S3 in the Supporting Information). The line width and density of immobilized structures can be tuned by adjusting the ac voltage source parameters such as peak-to-peak voltage and frequency, light source parameters such as light intensity and spot size, and operational parameters such as the exposure time and light pattern scanning speed. An example of this area density tuning is shown in Figure 1d where the number of patterned nanoparticles within the illuminated area is increased by increasing the exposure time from 2 to 120 s. After completion of the patterning process, the top ITO is removed and the remainder of the liquid is blow-dried leaving the patterned structures intact. The inset shows the scanning
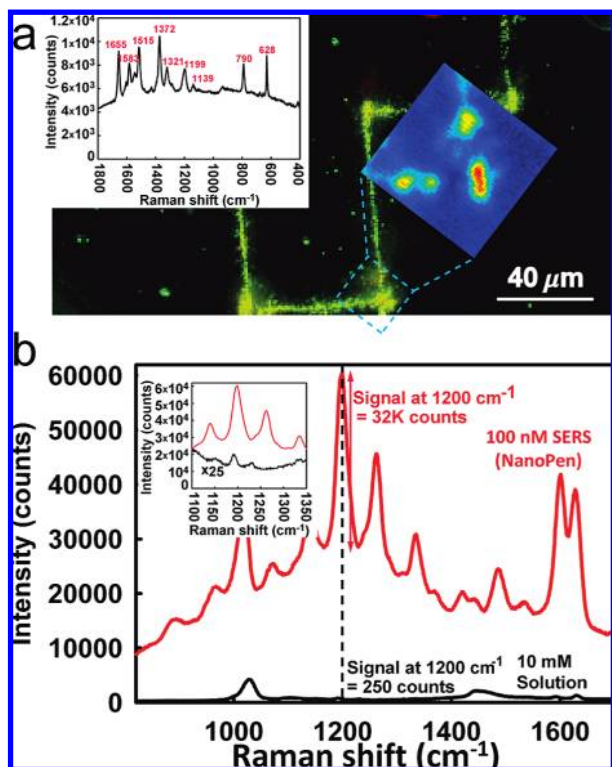
Figure 3. SERS using NanoPen patterned metallic nanoparticles. (a) Measurement of Rhodamine 6G (R6G) spectrum using the NanoPen patterned gold nanoparticle (mixture of 60 and 90 nm sizes). The two-dimensional scan of Raman signal at ~1570 cm^{-1} Raman shift indicated a large enhancement in the areas with higher density nanoparticles. The inset shows a typical Raman spectrum of R6G achieved. (b) Characterization of Raman enhancement factor for the BPE molecules. The Raman signal level is compared for 100 nM BPE solution on NanoPen SERS structures (red line) to the Raman signal from a benchmark 10 mM solution of BPE (black line). The inset shows a zoom-in of 1100−1350 cm^{-1} Raman shift range with the benchmark 10 mM solution signal multiplied by 25 to make it more visible. The calculated enhancement factor at the 1200 cm^{-1} Raman shift peak is ~10^7.

electron microscopy (SEM) image of the patterned spots, the number of particles patterned ranges from ~250 particles for a 2 s exposure to ~6500 particles for a 120 s exposure (see Figure S5 in the Supporting Information).

Since NanoPen is a light-induced patterning technique, it can be used for dynamic and flexible patterning of nanoparticles by adjusting the projected light pattern using a spatial light modulator. Moreover, the low required optical power intensity for actuation of NanoPen makes it possible to pattern the nanostructures using a commercial projector (Dell, 2400MP with 3000 ANSI Lumens, 1024 × 768 resolution) with <10 W/cm^2 optical intensity. To demonstrate this capability, we have patterned 90 nm diameter gold nanoparticles in the form of a 10 × 10 array over a 150 × 140 μm^2 area, the "NIH" logo over a 160 × 140 μm^2 area, and the "CAL" logo over a 140 × 110 μm^2 area, as shown in panels a, b, and c of Figure 2, respectively. These arbitrary patterns were created through a Microsoft Powerpoint interface with the projector. The optical patterns were then focused onto the OET chip using a 20× objective. The exposure time for 10 × 10 spot array is 2 min. The slight

nonuniformity in the patterns is due to the nonuniformity of the projected light patterns and could be improved through better optical alignment.

Applications of patterned nanostructures range from fabrication of opto- and nanoelectronic devices in the case of nanowires and carbon nanotubes[4,5] to DNA microarrays[1,2] depending on the type and characteristics of the patterned nanoparticles. In recent years, metallic nanocrystals have received much attention as local, subdiffraction limited nanosensors[3] for medical and chemical diagnosis and imaging, due to their interesting plasmonic properties. Therefore, NanoPen patterned metallic nanoparticles present a method for flexible and dynamic patterning of surface-enhanced Raman spectroscopy (SERS) sensing structures. To explore this capability further, we tried a solution of Rhodamine 6G (R6G) dye on the surface of an arbitrary NanoPen patterned structure (Figure 3a). The NanoPen patterned SERS substrates were prepared by patterning a solution of 60−90 nm gold nanoparticles on the OET surface using the NanoPen process. Once the patterning is complete, the top ITO cover glass is removed and the remaining liquid is blow-dried, leaving the patterned area intact. The two-dimensional Raman scan (at 1570 cm^{-1} Raman shift) of the structure indicates strong signal enhancement in the areas that nanoparticles are patterned. Moreover, we observe that positions with higher nanoparticle concentration (longer exposure time) show better enhancement relative to areas with lower particle density. A typical Raman signal achieved from R6G molecules (using a 3 mW, 532 nm laser excitation) is shown in Figure 3a inset. To quantify the SERS enhancement factor for NanoPen patterned gold nanoparticles, we dried 1−10 μL droplets of a 100 nM solution of *trans*-1,2-bis(4-pyridyl)ethene (BPE)[38] molecules on a patterned area, followed by a 2 min rinse with methanol and water. Raman measurements were then performed using a Raman setup built around an inverted TE2000 Nikon microscope. Objectives of 10×, 40×, or 60× were used to focus the laser source (785 nm, 30 mW) onto the sample and collect the Raman signal. As shown in Figure 3b, the enhancement factor is calculated by comparing the Raman signal intensities acquired from the 100 nM BPE molecules dried on the SERS structures to the Raman intensities acquired from a benchmark solution of 10 mM BPE. At the 1200 cm^{-1} Raman shift peak, the Raman intensity for 100 nM solution for the SERS structures is 32000 counts versus 250 counts for the 10 mM benchmark solution leading to an enhancement factor (EF) of

$$EF = \frac{32000}{250} \times \frac{10 \text{ mM}}{100 \text{ nM}} \approx 1.3 \times 10^7$$

Figure 3b inset shows a zoomed-in version of the Raman signal of the main plot in the range 1100−1350 cm^{-1}, with the 10 mM benchmark solution Raman signal multiplied by a factor of 25 to make it more visible. The BPE Raman signals were achieved for 4 s integration using a 30 mW, 785 nm laser source, and all signal levels are measured relative to the background. In addition, we observed a strong SERS signal with concentrations as small as picomolars (see Figure S6 in Supporting Information).

Currently, due to the small size of the patterned particles (<100 nm), the positioning accuracy is limited predominantly by Brownian motion and the diffraction-limited spot size. Moreover, NanoPen requires the use of a photoconductive thin-film substrate for the patterning process to work. However, after patterning the structures in the desired locations, the photoconductive film can potentially be removed[39] to allow further processing steps. In this work, we have focused on patterning one kind of a particle at a time. However, this limitation can be overcome through integration of NanoPen with microfluidic channels to form a complete optofluidic[40] system. Such integration would help realize promising applications such as the creation of DNA microarrys. However, future investigations need to be done to study the operational conditions of NanoPen for patterning biomaterials such as DNA and various proteins. Furthermore, since the immobilization force is dominated by the dielectrophoresis force, it can potentially be tuned according to particle size and material properties. In addition, the well-understood surface chemistry[41] of gold nanocrystals makes them ideal carriers of other materials such as DNA; therefore, NanoPen patterning of gold nanoparticles can be used to pattern other materials conjugated to the gold surface. In its present form NanoPen introduces a flexible, real-time reconfigurable, large-scale, and low-power method for patterning various nanostructures with potential applications in chemical and biological sensing, opto- and nanoelectronic device fabrication, nanostructure synthesis, and photovoltaics.

Supporting Information Available: Extensive figures on patterning a single Au nanoparticle, NanoPen patterning of one-dimensional structures such as multiwall carbon nanotubes and nanowires, patterning of nanoparticles with various surface charges, analysis of nanoparticle concentration in NanoPen patterned structures, and SERS detection of 10 pM concentration BPE molecules using NanoPen patterned Au nanoparticle structures. This material is available free of charge via the Internet at http://pubs.acs.org.

References

(1) Brown, P. O.; Botstein, D. *Nat. Genet.* **1999**, *21*, 33–37.
(2) Schena, M.; Shalon, D.; Davis, R. W.; Brown, P. O. *Science* **1995**, *270*, 467–470.
(3) Anker, J. N.; Hall, W. P.; Lyandres, O.; Shah, N. C.; Zhao, J.; Van Duyne, R. P. *Nat. Mater.* **2008**, *7*, 442–453.
(4) Huang, M. H.; Mao, S.; Feick, H.; Yan, H.; Wu, Y.; Kind, H.; Weber, E.; Russo, R.; Yang, P. *Science* **2001**, *292*, 1897–1899.
(5) Javey, A.; Guo, J.; Wang, Q.; Lundstrom, M.; Dai, H. *Nature* **2003**, *424*, 654–657.
(6) Yang, P. *MRS Bull.* **2005**, *30*, 85–91.
(7) Sun, B.; Findikoglu, A. T.; Sykora, M.; Werder, D. J.; Klimov, V. I. *Nano Lett.* **2009**, *9*, 1235.
(8) Piner, R. D.; Zhu, J.; Xu, F.; Hong, S.; Mirkin, C. A. *Science* **1999**, *283*, 661–663.
(9) Salaita, K.; Wang, Y.; Mirkin, C. A. *Nat. Nanotechnol.* **2007**, *145*, 145–155.
(10) Basnar, B.; Willner, I. *Small* **2009**, *5*, 28.
(11) Ginger, D. S.; Zhang, H.; Mirkin, C. A. *Angew. Chem., Int. Ed.* **2004**, *43*, 30.
(12) Li, B.; Goh, C. F.; Zhou, X.; Lu, G.; Tantang, H.; Chen, Y.; Xue, C.; Boey, F. Y. C.; Zhang, H. *Adv. Mater.* **2008**, *20*, 4873–4878.
(13) Wang, H. T.; Nafday, O. A.; Haaheim, J. R.; Tevaarwerk, E.; Amro, N. A.; Sanedrin, R. G.; Chang, C. Y.; Ren, F.; Pearton, S. J. *Appl. Phys. Lett.* **2008**, *93*, 143105.
(14) Hulteen, J. C.; Treichel, D. A.; Smith, M. T.; Duval, M. L.; Jensen, T. R.; Van Duyne, R. P. *J. Phys. Chem. B* **1999**, *103*, 3854–3863.
(15) Ahn, J. H.; Kim, H. S.; Lee, K. J.; Jeon, S.; Kang, S. J.; Sun, Y.; Nuzzo, R. G.; Rogers, J. A. *Science* **2006**, *314*, 1754–1757.
(16) Fan, Z.; Ho, J. C.; Jacobson, Z. A.; Yerushalmi, R.; Alley, R. L.; Razavi, H.; Javey, A. *Nano Lett.* **2008**, *8*, 20–25.
(17) He, H. X.; Li, Q. G.; Zhou, Z. Y.; Zhang, H.; Huang, W.; Li, S. F. Y.; Liu, Z. F. *Langmuir* **2000**, *16*, 9683.
(18) Xia, Y.; Whitesides, G. M. *Annu. Rev. Mater. Sci.* **1998**, *28*, 153.
(19) Yerushalmi, R.; Ho, J. C.; Jacobson, Z. A.; Javey, A. *Nano Lett.* **2007**, *7*, 2764–2768.
(20) Rabani, E.; Reichman, D. R.; Geissler, P. L.; Brus, L. E. *Nature* **2003**, *426*, 271–274.
(21) Collier, C. P.; Saykally, R. J.; Shiang, J. J.; Henrichs, S. E.; Heath, J. R. *Science* **1997**, *277*, 1978–1981.
(22) Hayward, R. C.; Saville, D. A.; Aksay, I. A. *Nature* **2000**, *404*, 56–59.
(23) Williams, S. J.; Kumar, A.; Wereley, S. T. *Lab Chip* **2008**, *8*, 1879–1882.
(24) Pauzauskie, P. J.; Radenovic, A.; Trepagnier, E.; Shroff, H.; Yang, P. D.; Liphardt, J. *Nat. Mater.* **2006**, *5*, 97–101.
(25) Ito, S.; Yoshikawa, H.; Masuharaa, H. *Appl. Phys. Lett.* **2001**, *78*, 2566–2568.
(26) Wilson, B. K.; Hegg, M.; Miao, X.; Cao, G.; Lin, L. Y. *Opt. Express* **2008**, *16*, 17276–17281.
(27) Chiou, P. Y.; Ohta, A. T.; Wu, M. C. *Nature* **2005**, *436*, 370–372.
(28) Jones, T. B. *Electromechanics of Particles*; Cambridge University Press: Cambridge, 1995.
(29) Ohta, A. T.; Chiou, P. Y.; Phan, H. L.; Sherwood, S. W.; Yang, J. M.; Lau, A. N. K.; Hsu, H. Y.; Jamshidi, A.; Wu, M. C. *IEEE J. Sel. Top. Quantum Electron.* **2007**, *243*, 235–243.
(30) Jamshidi, A.; Pauzauskie, P. J.; Schuck, P. J.; Ohta, A. T.; Chiou, P. Y.; Chou, J.; Yang, P. D.; Wu, M. C. *Nat. Photonics* **2008**, *2*, 85–89.
(31) Valley, J. K.; Jamshidi, A.; Ohta, A. T.; Hsu, H. Y.; Wu, M. C. *J. Microelectromech. Syst.* **2008**, *17*, 342–350.
(32) Chiou, P. Y.; Ohta, A. T.; Jamshidi, A.; Hsu, H. Y.; Wu, M. C. *J. Microelectromech. Syst.* **2008**, *17*, 525.
(33) Ramos, A.; Morgan, H.; Green, N. G.; Castellanos, A. *J. Colloid Interface Sci.* **1999**, *217*, 420–422.
(34) Castellanos, A.; Ramos, A.; Gonzalez, A.; Green, N. G.; Morgan, H. *J. Phys. D: Appl. Phys.* **2003**, *36*, 2584–2597.
(35) Ramos, A.; Morgan, H.; Green, N. G.; Castellanos, A. *J. Phys. D: Appl. Phys.* **1998**, *31*, 2338–2353.
(36) Lyklema, J. *Fundamentals of Interface and Colloid Science*; Academic: London, U.K., 1991; Vol. 2.
(37) Nanopartz, http://www.nanopartz.com/Spherical_Gold_Nanoparticles.htm, 2008.
(38) Yang, W.; Hulteen, J.; Schatz, G. C.; Van Duyne, R. P. *J. Chem. Phys.* **1996**, *104*, 4313–4323.
(39) Tien, M. C.; Ohta, A. T.; Yu, K.; Neale, S. L.; Wu, M. C. *Appl. Phys. A: Mater. Sci. Process.* **2009**, *95*, 967.
(40) Psaltis, D.; Quake, S. R.; Yang, C. *Nature* **2006**, *442*, 381–386.
(41) Daniel, M. C.; Astruc, D. *Chem. Rev.* **2004**, *104*, 293–346.

NL901239A